Dynamic patterns and ecological impacts of declining ocean pH in a high-resolution multi-year dataset

J. Timothy Wootton[1], Catherine A. Pfister, and James D. Forester[2]

Department of Ecology and Evolution, University of Chicago, 1101 East 57th Street, Chicago, IL 60637

Communicated by Robert T. Paine, University of Washington, Seattle, WA, October 8, 2008 (received for review August 8, 2008)

Increasing global concentrations of atmospheric CO_2 are predicted to decrease ocean pH, with potentially severe impacts on marine food webs, but empirical data documenting ocean pH over time are limited. In a high-resolution dataset spanning 8 years, pH at a north-temperate coastal site declined with increasing atmospheric CO_2 levels and varied substantially in response to biological processes and physical conditions that fluctuate over multiple time scales. Applying a method to link environmental change to species dynamics via multispecies Markov chain models reveals strong links between *in situ* benthic species dynamics and variation in ocean pH, with calcareous species generally performing more poorly than noncalcareous species in years with low pH. The models project the long-term consequences of these dynamic changes, which predict substantial shifts in the species dominating the habitat as a consequence of both direct effects of reduced calcification and indirect effects arising from the web of species interactions. Our results indicate that pH decline is proceeding at a more rapid rate than previously predicted in some areas, and that this decline has ecological consequences for near shore benthic ecosystems.

CO_2 | global change | ocean acidification | species interactions

There is accelerating and widespread interest in understanding and predicting the effects of the well-established increase of atmospheric CO_2, arising from fossil fuel burning, deforestation, and other human activities, on global climate and structure and function of ecosystems (1). Although much research on this topic has focused on terrestrial and atmospheric components, oceans play a significant role in global carbon cycles both through biological pathways (e.g., photosynthesis, respiration, sedimentation) and through the ubiquitous chemical reaction of CO_2 with water to create carbonic acid and its ionic products (2, 3). Much research has been focused on the process of CO_2 absorption from the atmosphere into the ocean, with special attention paid to the possible sequestration of carbon by photosynthesis, followed by sedimentation, and the possible impacts of changing temperature on oceans arising from the greenhouse effect of atmospheric CO_2. Recently, however, marine scientists have started to realize the substantial implications of declining pH (4, 5).

Changing pH levels potentially have vast consequences for marine ecosystems because of the critical role pH plays in mediating physiological reactions. Furthermore, many important groups of marine organisms have a skeleton of calcium-carbonate, which dissolves when it reacts with free hydrogen ions (5–8). Hence, declining pH could interfere with critical processes such as reef building, carbon sequestration via phytoplankton sedimentation, and consumer-resource interactions. Recent calculations indicate that increasing CO_2 concentrations may deplete the buffering capacity, in at least some parts of the ocean, and that ocean pH may drop 0.2 units over the next century (3, 9). Many sources now state that ocean pH has already changed 0.1 units over the past century (3, 10). The basis for these statements is model simulations that include only physical processes in the control of pH and that are calibrated from a single year of data (3) rather than those that use direct empirical measurements of ocean pH through time. Little published empirical information exists on the dynamics of directly measured ocean pH (1, 11), and none is available at temperate latitudes, which harbor the world's most productive fisheries.

In addition to understanding the dynamics of ocean pH, a key unanswered question is how marine ecosystems will respond to the anticipated declines in ocean pH (1, 12). From basic principles of biology and chemistry, calcifying organisms are expected to be impacted most negatively by decreasing pH. Laboratory experiments demonstrate that declining pH can negatively impact calcification in corals, mollusks, coralline algae, and phytoplankton (5–8), but laboratory experiments can be difficult to extrapolate to ecosystem responses because pH may affect other aspects of species biology besides calcification, and because the web of species interactions can enhance or counteract effects of environmental impacts (12–13). Here, we present detailed data on temporal variation of coastal ocean pH at a temperate site and relate it to suspected biological and physical drivers. We then introduce an approach that uses multispecies Markov chain models (14–15) that link pH change with extensive data on species dynamics to assess effects of pH on the structure and function of a coastal ecosystem.

Results

Examination of 24,519 measurements of coastal ocean pH spanning 8 years (Fig. 1) revealed several patterns. First, in contrast to the historical perspective that the ocean is well buffered, pH exhibited a pronounced 24-hour cycle, spanning 0.24 units during a typical day (Fig. 1*A*). This diurnal oscillation is readily explained by daily variation in photosynthesis and background respiration: water pH increases as CO_2 is taken up, via photosynthesis, over the course of the day, and then declines as respiration and diffusion from the atmosphere replenish CO_2 overnight (16). Second, pH fluctuated substantially among days and years, ranging across a unit or more within any given year and 1.5 units over the study period. Finally, when the entire temporal span of the data was considered (Fig. 1*B*), a general declining trend in pH became apparent.

A model of mechanistic drivers (supporting information (SI) Fig. S1) underlying changes in pH captured 70.7% of the variance in the data. All parameters differed significantly from zero (Table 1) after accounting for temporal autocorrelation (17). Relationships generally followed those expected based on known mechanisms likely to influence pH: pH declined as atmospheric CO_2 increased, fluctuated with available sunlight, increased with increasing phytoplankton abundance, decreased

Author contributions: J.T.W. and C.A.P. designed research; J.T.W. and C.A.P. performed research; J.T.W., C.A.P., and J.D.F. analyzed data; and J.T.W., C.A.P., and J.D.F. wrote the paper.

The authors declare no conflict of interest.

[1]To whom correspondence should be addressed. E-mail: twootton@uchicago.edu.

[2]Present address: Department of Organismic and Evolutionary Biology, Harvard University, 26 Oxford Street, Cambridge, MA 01238.

This article contains supporting information online at www.pnas.org/cgi/content/full/0810079105/DCSupplemental.

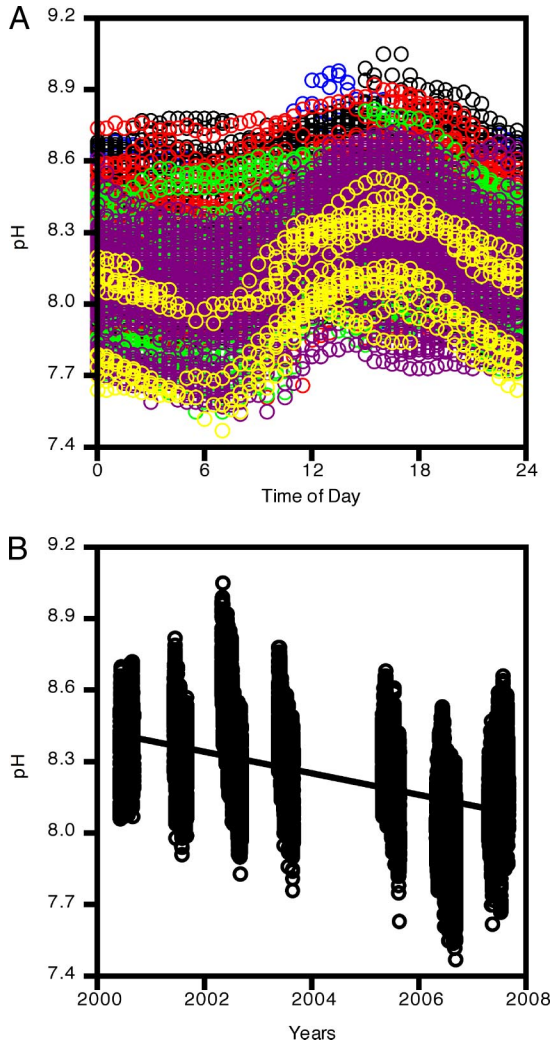

Fig. 1. Patterns of ocean pH through time at Tatoosh Island ($N = 24{,}519$). (*A*) Daily cycle of pH arising from photosynthetic uptake of CO_2 by algal primary producers. Colors indicate month that the data were collected (blue, April; black, May; red, June; green, July; purple, August; yellow, September). (*B*) pH readings as a function of date and time taken between 2000 and 2007. The decline is significant ($P < 0.05$).

with increasing upwelling, increased with increasing alkalinity, and increased with increasing water temperature. These results provide direct empirical support for the hypothesis that increasing atmospheric CO_2 levels reduce the pH in ocean surface waters, and also indicate that biological processes influence ocean pH and, hence, are important to incorporate into models of ocean pH.

Previous model predictions emphasize rates of change in ocean pH over time (3). Hence, we compared our empirical results to these predictions by fitting our pH data to a model with a linear temporal trend. The linear decline explained 23.9% of the variation in the data, and generated an estimated annual trend of −0.045 (95% C.I. −0.039 to −0.054 after accounting for temporal autocorrelation). This rate of decline is more than an order of magnitude higher than predicted by simulation models (−0.0019; ref. 3), suggesting that ocean acidification may be a more urgent issue than previously predicted, at least in some areas of the ocean.

Patterns of 10,356 annual transitions among species occupying 1,726 fixed points on rock benches within the mussel-dominated middle intertidal zone varied significantly across years during the study period (log-linear analysis, $G_{1183} = 4360.7$, $P < 0.0001$). Correlations between differences in annual transition and average annual pH (Fig. 2*A*) generally supported the hypothesis that declining pH reduces the performance of calcifying organisms (Fig. 2*B*): The correlation between pH and transition probabilities among species differed significantly between calcareous and noncalcareous taxa (t tests, all $P < 0.02$). Calcareous species exhibited increasing probabilities of replacement by other species as pH decreased and decreasing probabilities of displacing other species, whereas noncalcareous taxa exhibited the opposite response (Fig. 2*B*).

We explored the long-term consequences of annual variations in transitions related to pH change by using them as parameters in multispecies Markov chain models (14). The predictions derived from each annual set of transitions revealed systematic changes in community structure as a function of mean annual pH (Fig. 3*A*): the abundance and mean size of the dominant species in the system, the California mussel (*Mytilus californianus*), declined with declining pH, as did the blue mussel (*Mytilus trossulus*) and the goose barnacle (*Pollicipes polymerus*). In contrast, the abundance of acorn barnacles (*Balanus glandula*, *Semibalanus cariosus*) and fleshy algae (*Halosaccion glandiforme*, ephemeral algae, filamentous red algae, and foliose red algae) increased with declining pH.

We summarized the predictions of the Markov chain models by using principal components analysis, and then examined the association of the dominant principle component with high and low pH years. The dominant principle component (Fig. 3*B*) explained 48% of the variance in predicted species composition and was negatively associated with pH (Fig. 3*C*, linear regression, $P < 0.03$). The related species loadings were generally charac-

Table 1. Best-fit parameters for a model of ocean pH as a function of atmospheric CO_2, physical, and algal parameters

Parameter	Interpretation	Mean	95% C.I.	GR^2*
a	Constant, pH	15.948	31.659, 0.237†	–
b	Change in pH with atmospheric CO_2, pH/ppm CO_2	−20.593	−20.071, −21.114‡	29.8
h	Half the amplitude of the diurnal productivity oscillation, pH	−0.113	−0.108, −0.118†	25.3
φ	Phase shift from midnight of diurnal, h	2.380	2.536, 2.223†	
u	Effects of upwelling, pH/(metric tons/sec/100 m coastline)	−0.005	−0.005, −0.005‡	24.8
c	Phytoplankton abundance effect, pH-liter/mg chlorophyll	0.201	0.209, 0.192‡	13.8
τ	Temperature effect, pH/°C	0.078	0.084, 0.072†	8.9
d	Pacific Decadal Oscillation effect, pH/ °C	−0.045	−0.041, −0.049‡	2.7
k	Estimated Alkalinity, pH/μmol/kg	14.390	19.247, 9.534†	0.5
s	Salinity effect, pH/ppt dissolved salt	−0.112	−0.074, −0.150†	0.5

*Generalized R^2 (see *Methods*).
†$N_{adj} = 609.58$.
‡$N_{adj} = 24.11$.

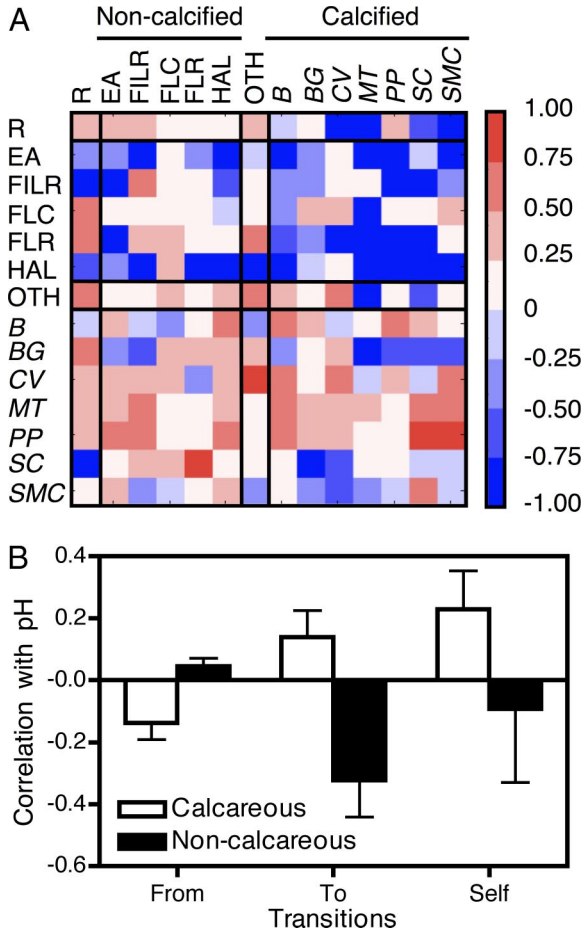

Fig. 2. Patterns of correlations between annual species replacement patterns at 1,726 fixed points in space and annual average pH during the year. (*A*) Matrix of correlations between average annual pH and transitions from the starting ecological state (columns) to the ecological state in the following year (rows), scaled by color for correlation coefficients ranging from 1 (bright red) to −1 (bright blue). Ecological states used in transition analysis (grouped by presence of a calcareous skeleton): B-big *Mytilus californianus*, BG-*Balanus glandula*, CV-*Corallina vancouveriensis*, HAL-*Halosaccion glandiforme*, MT-*Mytilus trossulus*, PP-*Pollicipes polymerus*, SC-*Semibalanus cariosus*, SMC-small *Mytilus californianus*, FILR-filamentous Rhodophytes, FLR-foliose Rhodophytes, FLC-fleshy crustose algae, R-rock and diatoms, EA-ephemeral algae (*Porphyra* and *Ulva* spp.), and OTH-other rare sessile species. Taxa with calcareous skeletons or shells indicated in italics. OTH category includes both calcareous and non-calcareous species. (*B*) Average correlation between average annual pH and annual transitions from a target species to another species (''From''), from another species to a target species (''To''), or the probability that a target taxon remains at a point in the following year (''Self''), as a function of whether the target taxon has a calcareous skeleton (□) or not (■).

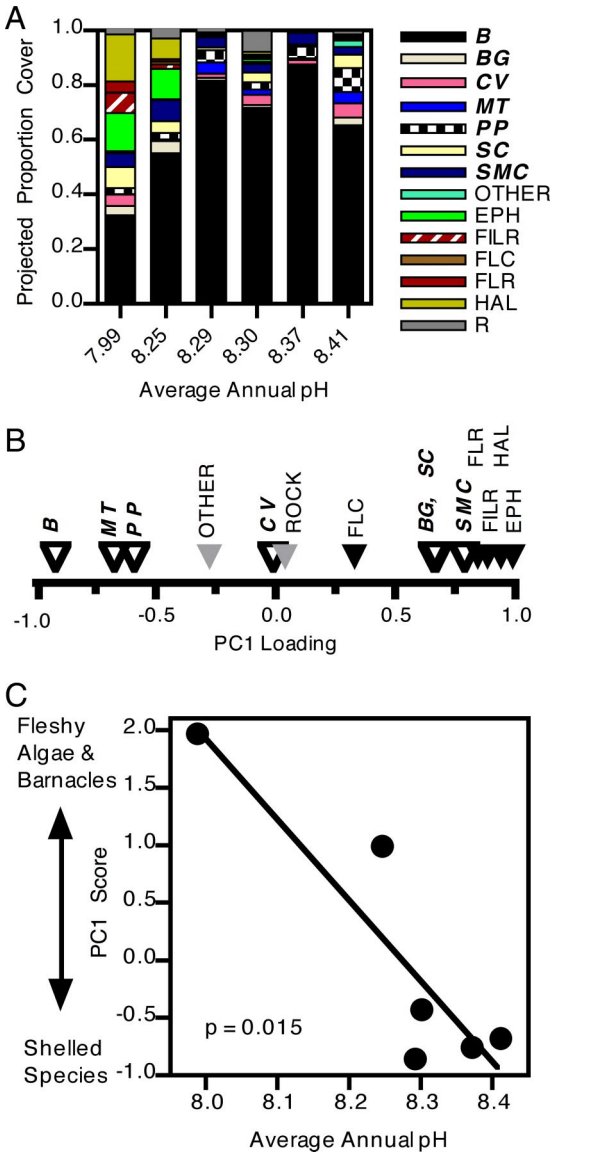

Fig. 3. Relationship between long-term predictions of sessile species composition derived from Markov chain models, parameterized from transitions in each year in relation to average annual pH. Taxon codes as in Fig. 2, with calcareous taxa indicated by bold italics. (*A*) Predicted taxa composition of each year, sorted by average pH in that year. (*B*) Taxon loadings of the first principle component, which describe annual variation in long-term predictions of taxon composition by Markov chain models. Open triangles are calcareous taxa. (*C*) Relationship between the first principle component that described long-term predictions of taxon composition by Markov chain models and the average annual pH.

terized by high positive values for fleshy algae and acorn barnacles, and low values for dominant calcareous species (Fig. 3*B*). Hence, Markov chain models predict that declining ocean pH will cause reductions in large dominant calcifying animals, little change in calcareous coralline algae, and increases in noncalcareous algae and subdominant calcareous acorn barnacles.

Discussion

Our data demonstrate that ocean pH exhibits strong dynamic patterns over multiple temporal scales, which can be linked to variation in key physical and biological drivers with known mechanistic ties to pH. Across years, pH declined strongly in association with increases in atmospheric CO_2. Over diurnal timescales, pH also showed strong systematic variation as a result of the interplay between uptake of CO_2 via photosynthesis and release of CO_2 via respiration. Ocean pH also exhibited variability at the seasonal time scale, but these patterns were more complex, with some years showing systematic increases and some showing systematic declines. This complexity is linked to annual variability in the seasonal patterns of drivers of pH (Fig. S1). Two factors tend to increase pH seasonally: atmospheric CO_2 declines during the summer as it is removed by terrestrial photosynthesis, and increased solar radiation tends to increase water temperature, which reduces CO_2 solubility. Two other factors tend to decrease pH seasonally: phytoplankton frequently decline through the summer (Fig. S1), reducing photosynthetic CO_2

uptake, and upwelling generally increases through the summer, which brings high concentrations of CO_2, arising from subsurface respiration, to the surface water, and also offsets seasonal increases in water temperature. In general, the effect of upwelling appears to predominate at the seasonal scale, but varies strongly among years. Although the Pacific Decadal Oscillation (PDO) index was negatively associated with pH and exhibited a large oscillation over the study period, it contributed relatively little to the explanatory ability of the model (<3%) compared with other variables (Table 1). This is, perhaps, because surface temperature and upwelling, two variables strongly linked to the index, are explicitly included in our model. Salinity and estimated alkalinity also contributed little to variation in pH (<1%), probably because salinity did not vary much over the study period. Overall, we have demonstrated the importance of incorporating both biotic and abiotic components into models of pH dynamics.

Our results agree qualitatively with predictions that ocean pH will decline with increases in atmospheric CO_2, but the rate of decline we observe is substantially faster than predicted by current models and exhibited by the limited data that exist on ocean pH change through time (1, 11). Our model includes all variables that are currently suggested to have a large impact on ocean pH (1, 18–20). Of these, only atmospheric CO_2 exhibits a consistent change that can explain the persistent decline in pH. These data are the only time series of ocean pH currently available for higher latitudes, hence, the associated changes in environmental conditions, such as high biological production and upwelling, may underlie the observed rapid decline, perhaps interacting with atmospheric CO_2 concentration in ways that are currently not well understood. Therefore, our results point to a need for more detailed investigation of processes controlling ocean pH in higher latitudes and coastal habitats.

Anticipating how marine ecosystems will respond to declining pH represents a major challenge. The approach we introduce here, using Markov chain models, provides a general way to link environmental change with the *in situ* dynamics of complex ecosystems and then predict long-term impacts on community structure. Prior research in our study system has rigorously tested the quantitative predictive ability of these models to novel conditions with field experiments (14, 21). In these studies, Markov chain models accurately anticipated experimental results, lending confidence to predictions made with this approach, particularly for the intertidal community in this study. Because many species are long-lived, which creates resistance to population change, and because small changes in ecological dynamics may take a long time to create large changes in population size, the use of Markov chain models to probe environmental impacts may be a more sensitive approach than classical indicator-species approaches to these problems.

The results of our analysis of ecological dynamics follow the general prediction that declining pH will negatively affect calcareous species, but the web of species interactions complicates the response. This complexity is demonstrated by the positive response to declining pH both by calcareous acorn barnacles and by noncalcareous fleshy algae, as well as the lack of response by the calcareous coralline algae, *Corallina vancouveriensis*. Prior experiments (21–23) provide convincing evidence that these species are strongly impacted by competition with the dominant calcareous sessile species whose performance declined with lower pH, as well as by predation and grazing by consumers with calcareous shells, which might also be impacted by lower pH. For example, the densities of grazing mollusks decline as pH declines ($r > 0.855$, $P < 0.05$). Algae may also benefit from elevated dissolved CO_2 concentrations. Hence, ecosystem-wide response to changing pH is neither a simple function of having calcareous body parts nor a general decline in organism performance. The qualitative patterns we observe among functional groups are strikingly similar to those reported in a study of marine communities around volcanic CO_2 seeps (12), suggesting such biotic changes might follow a general pattern. Anticipating the consequences of changing pH will require an understanding of both the physiological impacts of pH at the organismic level and the structure and function of interactions among ecosystem components.

Our data indicating impacts of changing pH on mussel-dominated communities are of interest for several reasons. *Mytilus californianus* mussel beds are a dominant coastal habitat along the northeastern Pacific, and mussel beds, in general, are an important habitat on most temperate rocky shores (24). These habitats provide food and structure for a diverse array of species in an otherwise physically stressful environment, and the dominant calcareous species provide food resources for humans. Mussels also impact coastal water conditions through their filtering activities and influences on nutrient recycling pathways (25). Compared with other biogenic habitats, such as coral reefs and sea grass beds, evidence of substantial impacts of global change on rocky intertidal habitats has been sparse. This is perhaps because intertidal organisms naturally endure harsh physical fluctuations and are predisposed to tolerate varying environmental conditions. Hence, our results indicating that these robust systems are impacted by changes in pH may portend much broader-scale impacts in other marine habitats.

In summary, our data demonstrate that coastal ocean pH is unexpectedly dynamic given the historical perspective that oceans are highly buffered, and shows that pH is declining in association with increases in atmospheric CO_2. Our results also provide clear links between pH and biological activity, which may be essential to incorporate when developing quantitative predictions of ocean pH in response to anthropogenic change. Qualitatively, however, our results support the broad predictions of physical models suggesting that ocean pH decline is an ongoing process. Our data also indicate that these changes are ecologically meaningful and merit further efforts to understand their causes and consequences by placing ocean pH change in a predictive framework for complex marine ecosystems. Collecting the intensive data needed to document high-resolution, long-term pH dynamics and their ecological impacts in the field necessarily limits the spatial extent of our study. For example, our study probes coastal surface waters, and, hence, may not reflect subsurface pH dynamics in the open ocean. The low pH values revealed in a recent spatial survey along the Pacific coast of North America (20) suggest, however, that the dynamics we report are broadly applicable. Although coastal and surface waters make up only a small portion of the world's oceans, they are focal points for ocean production and human activity; therefore, understanding pH changes in these areas is crucial. Our results highlight the urgent need for more spatially distributed and temporally intensive studies of ocean pH dynamics and their underlying causal mechanisms and consequences.

Methods

Study Site and Physical-Chemical Data Collection. As part of a larger effort to understand ecological dynamics, in 2000, we initiated a high-resolution monitoring program of selected physical-chemical water condition variables at Tatoosh Island (48.32 °N, 124.74 °W), using a submersible data logger. Tatoosh, located in the Eastern Pacific 0.7 km off the northwestern tip of Washington State, USA, has been the subject of intensive ecological investigation for nearly 40 years, which facilitates placing pH dynamics in an ecological context. We explored general patterns of pH through time, with a particular interest in whether there was any evidence of a sustained decline in pH over the study period as predicted by scenarios with increasing atmospheric CO_2 concentration (3).

Physical data were collected with a Hydrolab DataSonde 4a multi-probe (Hach Company, Loveland, Colorado, USA), which included probes for measuring temperature, salinity, and pH (26). The pH probe used a 3M KCl solution with saturated AgCl as the electrolyte in the reference cell, and was calibrated with pH 7 and 10 NIST standards. The multi-probe was bolted to the side of a 5,200-liter

tide pool that was separated, at low tide (< 80 cm above MLLW), from a 5-m vertical drop-off into the open ocean on the north side of the island, with a 1-m ledge. Tracer dye studies on calm days (≈1 m swell) showed that 90% of water in the pool is exchanged with the open ocean within 10 min, with the majority exchanged within 3 min. Exchange rates would be faster under typical higher-swell conditions. Simultaneous measurements of temperature, pH, salinity, and dissolved oxygen, between the pool and the adjacent ocean, revealed no statistically significant differences (Fig. S2), which were a consequence of the large pool size and high exchange rate with the ocean. Physical-chemical water condition variables were recorded at 30-min intervals from late spring/early summer to late summer, annually through 2007. The multi-probe was typically removed at approximately two-week intervals, coinciding with low spring tides, for maintenance and calibration, battery replacement, and data downloading. The multi-probe was replaced during the low tide of the following day.

We estimated surface alkalinity (A_T) from our measurements of water temperature and salinity by using the empirical relationships provided by Lee *et al.* (27) for the Northeast Pacific. We supplemented our physical data with information from web-accessible datasets on tide height that corresponded to the sampling time (http://tbone.biol.sc.edu/tide/index.html); monthly average values for atmospheric surface CO_2 concentrations measured at the NOAA Earth System Research Laboratory (P. Tans; http://www.esrl.noaa.gov/gmd/ccgg/trends); upwelling at 48°N 25°W, as estimated from NOAA surface wind measurements (http://www.pfeg.noaa.gov); and PDO (http://jisao.washington.edu/pdo) and Sea-viewing Wide Field-of-view Sensor (SeaWiFS) estimates of chlorophyll concentration (http://coastwatch.pfel.noaa.gov). SeaWiFS satellite data were taken from a block of ocean (48°22′–48°26′N; 124°43′–124°47′W) encompassing Tatoosh Island and the ocean immediately to the northwest of the island, which lacks interfering land signals and is less regularly impacted by fog.

Statistical Analysis and Modeling of pH. Given current understanding of key factors affecting pH and CO_2 in the ocean, we developed a semimechanistic model to examine potentially important influences on pH dynamics and fit it to the observed data by using nonlinear regression. Our model was:

$$\begin{aligned}\mathrm{pH} = {} & a + b^{*}\log[CO_{2,atm}] + h^{*}\sin(2^{*}\pi^{*}(\varphi \\ & + Time\ of\ Day)/24) + u^{*}Upwelling \\ & + c^{*}\log(Chlorophyll) + \tau^{*}(Water\ Temperature) \\ & + d^{*}PDO + k^{*}\log(Alkalinity) + s^{*}Salinity \qquad [1]\end{aligned}$$

The model terms and their interpretation were as follows. A constant (*a*) set the starting conditions in 2000. The second term (*b*) described the trend in pH as a function of increasing atmospheric CO_2. This covariate was based on globally averaged marine surface level measurements, and was log-transformed to match the log scale of pH. This relationship was predicted to be negative (3). The third term accounted for diurnal oscillations arising from sun-driven fluctuations in photosynthesis, which was described by amplitude (h) and location (φ) parameters. The fourth term (τ) described the effect of water temperature (°C) on pH, which was expected to be positive because less CO_2 can be dissolved in water at higher temperatures. The fifth term (u) described the response of pH to upwelling. Upwelling could affect surface pH either by providing calcium from the deep-sea floor, resulting in a positive relationship as a result of increased buffering capacity, or by bringing to the surface water with high dissolved concentrations of CO_2 that arise from respiration in the aphotic zone, resulting in a negative relationship. The sixth term described the effects of variation in regional phytoplankton abundance on pH, as estimated by SeaWiFS satellite-based surface color estimates. These data were also log-transformed to match the log scale of pH. Increasing phytoplankton populations should take up larger amounts of CO_2, thereby increasing pH. The seventh term relates pH to the PDO. An index associated with the PDO was identified as the primary driver of the pH changes inferred from mineral markers at a coral reef site (19). The eighth term relates pH to the log of estimated alkalinity in the surface waters. Increasing alkalinity should offset production of carbonic acid, leading to a positive relationship with pH. The last term accounted for any dependence of measured pH on the water salinity (ppt), independent of its effects on alkalinity.

We analyzed data by using least squares nonlinear regression routines in SPSS 16.0.1 and R 2.6.2 statistical software to fit equation (1) to our data. To ensure that our measures reflected oceanic conditions, we only included data taken when the sampling site was physically connected to the ocean (i.e., tide height >80 cm above Mean Lower Low Water (MLLW). To improve our measurement precision, we also statistically controlled for any sensor drift by deriving from the data a general relationship between change in measured pH and time since calibration using nonlinear regression. In 2004, the pH sensor acted erratically and then completely failed, and was not replaced until the end of the field season, so we omitted this year from the analysis. Analysis with 2004 yielded similar parameter estimates, but residuals behaved poorly because the 2004 data were outliers. We also omitted data points where one or more other physical variables (typically SeaWiFS chlorophyll estimates) was missing, and a few outliers in our salinity data where readings jumped to unrealistically low levels and immediately returned to typical values within the high resolution time series. After these procedures, 19,364 measurements of the original 36,352 remained. Data series for parameters other than pH are presented in Fig. S1. The relative importance of each covariate was assessed by comparing the full model to models reduced by one parameter (or, in the case of the diurnal oscillation, two parameters) via the generalized R^2 statistic (GR^2, ref. 28). This statistic is calculated as: $GR^2 = 1 - \Sigma(RSS_{full\ model})/\Sigma(RSS_{reduced\ model})$ and represents the reduction in explained variance when a given variable is removed from the full model.

Temporal autocorrelation presents a problem when statistically testing hypotheses and constructing parameter confidence intervals with regression because data points are not independent, resulting in inflated degrees of freedom. To address this problem, we used Trenberth's (17) method for estimating an autocorrelation-adjusted sample size, $N_{adj} = N/(1 + 2^{*}(1–1/N)^{*}AC_1)$, where N is the sample size, N_{adj} is the adjusted sample size, and AC_1 is the first-order autocorrelation of the residuals, which we estimated by using autocorrelation analysis of the data ordered in temporal sequence. This method is based on the expected number of sequential samples required for the effects of first-order autocorrelations to dampen to near zero, hence, the inverse yields an estimate of the effective sample size of the dataset. The data we analyzed were taken at two resolutions (every half hour or monthly averages), so estimated sample sizes and degrees of freedom were adjusted accordingly (*i.e.*, N = 19,364 for half-hourly data, N = 26 for monthly averages), and first-order autocorrelations were calculated with either model residuals or monthly averages of residuals, respectively, to generate autocorrelation adjusted sample sizes for all degrees of freedom calculations. We checked the robustness of our results using an alternative approach, in which we only analyzed small subsets of the data spaced 900 points apart in the sequence, to reduce autocorrelation. These analyses yielded similar results (Table S1).

Ecological Dynamics Data. Concurrent with our collection of physical characteristics of the ocean, we continued long-term detailed studies of species dynamics in this system. We took advantage of the large variation in pH across our study period to gain insight into the likely impacts of declining ocean pH on near shore community structure. Specifically, we collected detailed data on annual patterns of species replacements at this site (14, 29), which may provide a much more sensitive picture of important processes affecting this ecosystem than traditional indicator species approaches.

Details of the biological sampling scheme and application to Markov chain models are presented in (14). Beginning in 1993, species transitions were derived from 14 permanent 60 × 60-cm quadrants containing 100 fixed points each, and from 11 permanent transects containing 30 randomly selected fixed points. Four points on the transects were not sampled because they occurred over crevices in the rock or in transect hardware. In late spring of each year, each point was surveyed for its ecological state, which was identified by bare space or the species identity of the individual that was present. Overall, our analysis described the transition patterns among 14 ecological states, which are reported in Fig. 2 and in prior studies (14, 21).

Ecological Dynamics Modeling and Analysis. Annual transitions among species or broader functional groups were derived by generating a matrix of frequencies of the state of each point at a census (columns) with its state in the census of the following year (rows), and then generating a transition matrix by dividing each element by the sum of its column. We tested for variation in transitions among years by applying log-linear contingency table analysis to the transition frequency matrix:

$$-2\cdot\ln(\lambda) = 2\cdot\sum_{i=1}^{s}\sum_{j=1}^{s}\sum_{t=2000}^{2007} n_{t,ij}\cdot\ln(p_{t,ij}/\bar{p}_{ij}) \qquad [2]$$

where $n_{t,ij}$ is the element from state i to state j in the transition frequency matrix from year t; $p_{t,ij}$ is the element from state i to state j in the transition probability matrix from year t ($t \neq 2004$); s = 14 is the total number of ecological states, and p_{ij} is the transition from state i to state j in the transition probability matrix derived from transition data across all years. We tested this statistic against a χ^2 distribution with 1183 degrees of freedom (15). Using Pearson correlation coefficients, we probed whether any detected variation in

transition patterns was related to pH change by correlating the annual variation in each transition probability with the average annual pH measured in the intervening year. Because prior discussion of pH impacts on marine systems has emphasized effects of calcium carbonate dissolution (5–8), we tested whether associations between transitions and ocean pH varied between taxa with calcium carbonate skeletons (mollusks, barnacles, and coralline algae) and taxa without calcium carbonate skeletons (fleshy algae). The rare taxa category was not included in the analysis because this group contained both calcifying and noncalcifying species. We compared patterns in transitions both to (displacement/colonization ability) and from (replacement resistance) the focal taxa using t tests. Compared with noncalcifying species, we predicted more negative associations for transitions from calcifiers to other taxa and more positive associations for transitions from other taxa to calcifiers.

To assess the long-term implications of differences in transitions among years on the composition of the intertidal community, we used each annual transition matrix as a parameter in a multispecies Markov Chain community model (14–15). We projected the long-term composition, implied by the set of transitions observed in each year, by finding the eigenvector associated with the dominant eigenvalue of the matrix and standardizing it so that the sum of the elements = 1. We then summarized the variability of the predicted long-term compositions, implied by transitions derived from each year, using principle components analysis that used component loadings of individual taxa to interpret dominant axes. Because the first principle component captured almost half the annual variance in predicted long-term community structure, we focused our analysis on this component. To test whether ocean pH was associated with predicted long-term species composition, we used linear regression between average pH and the first principle component score for each year. We also used multidimensional scaling and obtained similar results.

ACKNOWLEDGMENTS. We thank the Makah Tribal Council for granting access to Tatoosh Island and K. Barnes, J. Duke, K. Edwards, A. Gehman, A. Kandur, R. Kordas, B. Linsay, H. Lutz, C. Neufeld, A. Norman, M. Novak, J. Orcutt, R. Paine, K. Rose, K. Weersing, A. Weintraub, L. Weis, A. Wootton, and B. Wootton for assisting with the fieldwork. Funding was provided in part by the Andrew W. Mellon Foundation, the Olympic Natural Resources Center, and National Science Foundation Grants OCE 97-11802, OCE 01–17801, and OCE 04-52678.

1. Solomon S, *et al.* (2007) *Climate Change 2007: The Physical Science Basis. Contribution of Working Group I to the Fourth Assessment. Report of the Intergovernmental Panel on Climate Change* (Cambridge Univ. Press, Cambridge, UK).
2. Millero FJ (2007) The marine inorganic carbon cycle. *Chem Rev* 107:308–341.
3. Orr JC, *et al.* (2005) Anthropogenic ocean acidification over the twenty-first century and its impact on calcifying organisms. *Nature* 437:681–686.
4. Broecker WS, Takahashi T, Simpson HJ, Peng TH (1979) Fate of fossil fuel carbon dioxide and the global carbon budget. *Science* 206:409–418.
5. Kleypas JA, *et al.* (1999) Geochemical consequences of increased atmospheric carbon dioxide on coral reefs. *Science* 284:118–120.
6. Feely RA, *et al.* (2004) Impact of anthropogenic CO_2 on the $CaCO_3$ system in the oceans. *Science* 305:362–366.
7. Gao K, *et al.* (1993) Calcification in the articulated coralline alga *Corallina pilulifera*, with special reference to the effect of elevated CO_2 concentration. *Mar Biol* 117:129–132.
8. Riebesell U, *et al.* (2007) Enhanced biological carbon consumption in a high CO_2 ocean. *Nature* 450:545–549.
9. Caldiera K, Wickett ME (2003) Anthropogenic carbon and ocean pH. *Nature* 425:365.
10. Raven J, *et al.* (2005) *Ocean acidification due to increasing atmospheric carbon dioxide* (The Royal Society, London).
11. Santana-Casiano MJ, González-Dávila M, Rueda MJ, Llinás O, González-Dávila EF (2007). The interannual variability of oceanic CO_2 parameters in the northeast Atlantic subtropical gyre at the ESTOC site. *Global Biogeochem Cycles* 21:10.1029/2006GB002788.
12. Hall-Spencer JM, *et al.* (2008) Volcanic carbon dioxide vents show ecological effects of ocean acidification. *Nature* 454:95–99.
13. Schindler DW, *et al.* (1985) Long-term ecosystem stress - the effects of years of experimental acidification on a small lake. *Science* 228:1395–1401.
14. Wootton JT (2001) Prediction in complex communities: Analysis of empirically-derived Markov models. *Ecology* 82:580–598.
15. Caswell H (2001) *Matrix Population Models* (Sinauer, Sunderland).
16. Bensoussan N, Gattuso JP (2007) Community primary production and calcification in a NW Mediterranean ecosystem dominated by calcareous macroalgae. *Mar Ecol Prog Ser* 334:37–45.
17. Trenberth KE (1984) Some effects of finite sample size and persistence on meteorological statistics. Part I: Autocorrelations. *Mon Wea Rev* 112:2359–2368.
18. Dore JE, Lukas R, Sadler DW, Karl DM (2003) Climate-driven changes to the atmospheric CO_2 sink in the subtropical North Pacific Ocean. *Nature* 424:754–757.
19. Pelejero C, *et al.* (2005) Preindustrial to modern interdecadal variability in coral reef pH. *Science* 309:2204–2207.
20. Feely RA, Sabine CL, Hernandez-Ayon JM, Ianson D, Hales B (2008) Evidence for upwelling of corrosive ''acidified'' water onto the continental shelf. *Science* 320:1490–1492.
21. Wootton JT (2004). Markov chain models predict the consequences of experimental extinctions. *Ecol Lett* 7:653–660.
22. Dayton PK (1971) Competition, disturbance, and community organization: The provision and subsequent utilization of space in a rocky intertidal community. *Ecol Monogr* 41:351–389.
23. Paine RT, Levin SA (1981) Intertidal landscapes: Disturbance and the dynamics of pattern. *Ecol Monogr* 51:145–178.
24. Stephenson TA, Stephenson A (1972) *Life between tidemarks on rocky shores* (Freeman, San Francisco, CA).
25. Pfister CA (2007) Intertidal invertebrates locally enhance primary production. *Ecology* 88:1647–1653.
26. Pfister CA, Wootton JT, Neufeld CJ (2007) The relative roles of coastal and oceanic processes in determining physical and chemical characteristics of an intensively sampled nearshore system. *Limnol Oceanogr* 52:1767–1775.
27. Lee K, *et al.* (2006) Global relationships of total alkalinity with salinity and temperature in surface waters of the world's oceans. *Geophys Res Lett* 10.1029/2006GL027207.
28. Anderson-Sprecher R (1994) Model comparisons and R^2. *Am Stat* 48:113–117.
29. Wootton JT (2005) Field-parameterization and experimental test of the Neutral Theory of Biodiversity. *Nature* 433:309–312.